Model-Predictive-Control-Based Path Tracking Controller of Autonomous Vehicle Considering Parametric Uncertainties and Velocity-Varying

Shuo Cheng, Liang Li, *Senior Member, IEEE*, Xiang Chen, Jian Wu, and Hong-da Wang

***Abstract*—The automated steering control technology is crucial for an autonomous vehicle, but due to parametric uncertainties and time varying, the performance of automated steering control can be degraded. Therefore, a vehicle automated steering controller based on a model predictive control (MPC) approach is proposed in this article. First, considering tire nonlinear characteristics, the state and control matrices are modified, then the time-varying vehicle speed is considered and a linear parameter varying lateral model is established through utilizing a polytope with finite vertices to describe vehicle longitudinal velocity. Then, the MPC-based vehicle path tracking controller, which is robust against parameter uncertainties, is designed; the proposed controller can be solved via a set of linear matrix inequalities (LMI), which are derived from Lyapunov asymptotic stability and the minimization of the worst case infinite horizon quadratic objective function. The proposed control system is evaluated by both cosimulations of MATLAB/Simulink & CarSim and real-bus tests. Results show the effectiveness of the proposed controller, and it can ensure the control accuracy and strong robustness.**

***Index Terms*—Automated steering system, linear matrix inequalities (LMI), parametric uncertainties, robust model predictive control (MPC).**

I. Introduction

ACCORDING to the statements of the World Health Organization (WHO) in recent years, about 1.25 million people die every year because of traffic accidents [1]. Drivers' improper maneuver and fatigue driving are main causes of various severe traffic accidents. Recently, the advanced driver assistance systems (ADAS) or even autonomous driving has been developed rapidly, and it is regarded as a solution to reduce drivers' errors and then decrease traffic injuries [2], [3]. Therefore, autonomous vehicles are widely considered as the mainstream of automakers, and many researchers have studied autonomous vehicle technologies a lot. ADAS has been applied in production cars in recent years, for instance, electronic stability control (ESC) [4], [5], autonomous emergency brake [6], adaptive cruise control [7], and lane deviation warning system [8], while the lateral control of an autonomous vehicle still needs to be further researched due to its great study difficulties.

The lateral control of an autonomous vehicle aims to make the ego vehicle track its desired trajectories automatically through steering wheel control, and ensures its robustness against various vehicle velocities, road conditions, and so on [9]. Some researchers focused on the active front steering system (AFS). AFS can make use of the front steering command in order to improve lateral vehicle stability, and add an extra angle to the driver's steering angle [10], [11]. Zhang and Wang [12] investigated the actuator fault detector design problem for an electric ground vehicle equipped with the AFS system. Wu *et al.* [13] proposed a sliding-mode-control (SMC)-based AFS control system, which considers the road adhesion constraint on vehicle stability. Previous works have also made great progress on coordination between AFS and some other chassis subsystems such as direct yaw moment control and active suspension system (ASS) [14]–[16]. A nonlinear model predictive control (MPC) method integrating AFS and an additional yaw moment was proposed by Guo *et al.* [17]. Then, a novel human–machine-cooperative-driving controller with a hierarchical structure for vehicle dynamic stability was proposed by Wu *et al.* [11].

Path tracking for an autonomous vehicle requires steering system control and accurate execution of the steering angle, which can be actualized by the steer-by-wire (SBW) technology. SBW cancels the mechanical connection between the steering wheel and tires and completely gets rid of the restrictions from the tradition steering system [18]. Setlur *et al.* [19] proposed a trajectory tracking SBW control system for the vehicle's position/orientation using a simplified vehicle description and reference model, and it is also a continuous time-varying tracking controller. Sun *et al.* [20] proposed a sliding-mode-based active disturbance rejection control scheme for a SBW system in road vehicles. The SBW system is a proper solution to the

Manuscript received January 15, 2020; revised March 20, 2020 and May 20, 2020; accepted July 8, 2020. Date of publication July 21, 2020; date of current version June 16, 2021. This work was supported in part by the Key Scientific and Technological Research Project in Anhui Province under Grant JAC2019022505 and in part by the National Science Fund of the People's Republic of China under Grant 51675293. *(Corresponding author: Xiang Chen.)*

Shuo Cheng, Liang Li, and Xiang Chen are with the State Key Laboratory of Automotive Safety and Energy, Tsinghua University, Beijing 100084, China (e-mail: chengs16@mails.tsinghua.edu.cn; liangl@mail.tsinghua.edu.cn; tschenxiang@mail.tsinghua.edu.cn).

Jian Wu is with the School of Mechanical and Automotive Engineering, Liaocheng University, Liaocheng 252000, China (e-mail: wujian@lcu.edu.cn).

Hong-da Wang is with the Zhongtong Bus Co., Ltd, Liaocheng 252000, China (e-mail: 15166506773@163.com).

Color versions of one or more of the figures in this article are available online at https://ieeexplore.ieee.org.

Digital Object Identifier 10.1109/TIE.2020.3009585

trajectory-following problem. The trajectory-following problem is very crucial for autonomous vehicles, and it has attracted many researchers' interests, many control algorithms have been designed such as MPC [21], [22], fuzzy controller [23], [24], SMC [20], [24], and linear quadratic regulator (LQR) [25].

While parametric uncertainties, time varying, and tire nonlinear characteristics bring great challenge to vehicle control, and some researchers have devoted themselves to tackle related issues. Great progress has been made on linear parameter varying modeling (LPV) and H-infinity control [26]–[28]. A new LPV/H-infinity control for active suspensions with performance adaptation was proposed by Zin *et al.* [27]. Furthermore, to improve vehicle comfort and safety, a novel LPV/H-infinity-based global chassis control including vehicle suspension, braking, and steering systems was proposed, and vehicle speed as a varying parameter was considered in LPV modeling [26]. Moreover, a new robust MPC, which allows explicit incorporation of the description of plant uncertainty in the problem formulation, was presented in [29], and then, Wan and Kothare [30] proposed an efficient offline formulation of MPC using linear matrix inequality (LMI). Khooban *et al.* [31] presented a novel Takagi–Sugeno fuzzy model-based MPC structure utilizing LMI for vehicle speed control including time-delay states and parameter uncertainty.

Considering the presence of the uncertainties mentioned above, Chen *et al.* [32] designed a hierarchical controller with an adaptive law to track a reference path. Besides, the lateral motion is hard to control since it is under actuated, nonlinear, and with large uncertainties [9]. Thus, a tracking control method based on active disturbance rejection control and differential flatness theory was proposed by Xia *et al.* [9]. Hwang *et al.* [24] presented a hierarchically improved fuzzy dynamical SMC to address the autonomous ground vehicle path tracking problem. Zhang *et al.* [33] first proposed a general T–S fuzzy lateral dynamic model taking the variations of vehicle mass and longitudinal velocity, and the nonlinearity of lateral tire and road force was described by a norm-bounded uncertainty.

However, the path tracking issues still need to be studied a lot. Due to parametric uncertainties and tire nonlinear characteristics [34], we focus on the path tracking control design for self-driving vehicles, which can ensure the accuracy of trajectory-following and its robustness. First, considering tire nonlinear characteristics, the state and control matrices are modified, then uncertain vehicle speed is considered in the vehicle lateral dynamics model and a LPV lateral model is established through utilizing a polytope with finite vertices to describe vehicle longitudinal velocity. Then, the MPC-based vehicle path tracking system, which is robust against parameter uncertainties is derived, the proposed controller can be solved via a set of LMI, which are derived from Lyapunov asymptotic stability and the minimization of the worst case infinite horizon quadratic objective function. Finally, the proposed controller is evaluated by both cosimulations of MATLAB/Simulink & CarSim and real-bus tests. The rest of this article is organized as follows. Section II presents there related models. Section III gives a detailed description about the design of the LMI-based MPC controller. In Section IV, its performance is tested by CarSim-MATLAB/ Simulink cosimulation and real-bus-tests. Finally, Section V concludes this article.

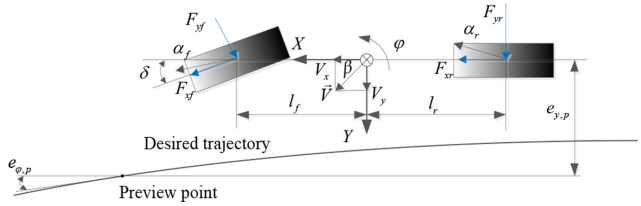

Fig. 1. Vehicle lateral dynamics and path-tracking model.

II. Dynamics Modeling and Problem Formulation

A. Vehicle Lateral Dynamics

Due to tire nonlinear characteristics, parametric uncertainties, and time-varying parameters, it is difficult to establish a vehicle model without some simplification assumptions. Moreover, the controller stability analysis and synthesis could be more complex with a more comprehensive vehicle model. In this article, an extensively utilized vehicle lateral model is adopted. To ensure the accuracy and robustness of the path-tracking controller, tire nonlinear characteristics and uncertainties, and time-varying velocity are considered to the modify vehicle lateral model.

The autonomous vehicle is a nonlinear and time-varying system. We assume that, first, discount the actuator dynamics systems (brake, throttle, and steering, etc.)and, second, neglect vehicle roll, pitch, and vertical motions. Then, the two-degree-of-freedom (2DOF) single-track vehicle model, as shown in Fig. 1, can be described, as shown in (1), and it has been extensively used for vehicle stability and vehicle dynamics state control. (X, Y) are inertial coordinates of the location of vehicular center of gravity, l_f and l_r are the distance from the vehicular center of gravity to the front and rear axle, respectively. m is the vehicle mass, and I_z is the yaw moment of inertia.

$$\begin{cases} m(\dot{V}_y + V_x\varphi) = F_{yf}\cos\delta + F_{xf}\sin\delta + F_{yr} \\ I_z\dot{\varphi} = l_f F_{yf}\cos\delta + l_f F_{xf}\sin\delta - l_r F_{yr} \end{cases} \tag{1}$$

where V_x and V_y denote the longitudinal and lateral velocity, respectively, and φ is the yaw rate. F_{xf} and F_{xr} denote the longitudinal force of vehicle front axle and rear axle, respectively. F_{yf} and F_{yr} the lateral force of vehicle front axle and rear axle, respectively. δ is the front wheel steering angle.

As shown in Fig. 1, the vehicle lateral kinematic model could be analyzed based on the relative position between the desired trajectory and vehicle location. $e_{y,p}$ represents the lateral error, which is the distance from the current vehicle position to the desired reference trajectory at the preview point, $e_{\varphi,p}$ denotes the relative angular error between the vehicular heading and the road tangent at a certain preview look-ahead distance. The proper preview distance could be calculated based on the vehicle speed by setting a preview time T_{pre} [35]. The derivative of the lateral error $e_{y,p}$ can be expressed as follows:

$$\dot{e}_{y,p} = \sin(e_{\varphi,p})V_x - V_y - \varphi D_p. \tag{2}$$

Due to the fact that the relative angular error is usually assumed as a small value, which is utilized in vehicular lateral control of autonomous vehicles, we can define that $\sin(e_{\varphi,p}) \approx e_{\varphi,p}$ [9]. Then, the vehicle lateral kinematic model for path-tracking

can be described as follows:

$$\begin{cases} \dot{e}_{y,p} = e_{\varphi,p}V_x - V_y - \varphi D_p \\ \dot{e}_{\varphi,p} = -\varphi + V_x\rho_p \end{cases} \tag{3}$$

where D_p denotes the preview look-ahead distance. ρ_p represents the curvature of the desired trajectory at the preview point.

B. Polytopic Uncertainty-Based Vehicle Model

The tires operate in the linear region when a vehicle runs with a small lateral acceleration. If we use the simple lateral tire force description mentioned above, i.e., the linear tire model. The lateral forces can be calculated by adopting the equivalent tire cornering stiffness k_f and k_r, as shown in the following equation:

$$\begin{cases} F_{yf} = k_f\alpha_f \\ F_{yr} = k_r\alpha_r \end{cases} \tag{4}$$

where side-slip angles of front and rear axles α_f and α_r can be approximated as follows:

$$\begin{cases} \alpha_f = \delta - \frac{V_y}{V_x} - \frac{\varphi l_f}{V_x} \\ \alpha_r = \frac{\varphi l_r}{V_x} - \frac{V_y}{V_x}. \end{cases} \tag{5}$$

The vehicle model presented in (1) can be rewritten as a state-space form by considering (4):

$$\dot{\mathbf{x}}_v = A_v\mathbf{x}_v + B_v u \tag{6}$$

where $\mathbf{x}_v = [V_y\ \varphi]^T$, u denotes front-wheel steering angle in radian, the system and control matrices A_v, B_v are as follows:

$$A_v = \begin{bmatrix} a_{11} & a_{12} \\ a_{21} & a_{22} \end{bmatrix} = \begin{bmatrix} \frac{k_f+k_r}{mV_x} & \frac{l_fk_f-l_rk_r}{mV_x} - V_x \\ \frac{l_fk_f-l_rk_r}{I_zV_x} & \frac{l_f^2k_f+l_r^2k_r}{V_xI_z} \end{bmatrix}$$

$$B_v = \begin{bmatrix} b_1 \\ b_2 \end{bmatrix} = \begin{bmatrix} -\frac{k_f}{m} \\ -\frac{l_fk_f}{I_z} \end{bmatrix}. \tag{7}$$

The following state-space equation can be derived by combining the vehicle lateral kinematic model, as shown in (3), and the vehicle lateral dynamics model, as shown in (7). The state-space equation containing vehicle kinematic and dynamics models can be expressed as follows:

$$\dot{\mathbf{x}}(t) = A(t)\mathbf{x}(t) + B(t)u(t) + F(t)w(t) \tag{8}$$

where $\mathbf{x} = [e_{y,p}\ e_{\varphi,p}\ V_y\ \varphi]^T$. The system and control matrices A are B are as follows:

$$A(t) = \begin{bmatrix} 0 & V_x & -1 & -D_p \\ 0 & 0 & 0 & -1 \\ 0 & 0 & a_{11} & a_{12} \\ 0 & 0 & a_{21} & a_{22} \end{bmatrix} \tag{9}$$

$$B(t) = \begin{bmatrix} 0 \\ 0 \\ b_1 \\ b_2 \end{bmatrix}, F(t) = \begin{bmatrix} 0 \\ V_x \\ 0 \\ 0 \end{bmatrix}, w(t) = \rho_p. \tag{10}$$

Due to tire nonlinear characteristics, it is difficult to obtain lateral tire forces exactly, especially when the lateral acceleration or side-slip angles are pretty large. As we all know, the cornering stiffness can be influenced by tire pressure, vertical tire force, and camber angle, so that its value is uncertainty. To illustrate lateral forces accurately, this article designs that the cornering stiffness changes between the range from 180 to 400 kN/rad generally. Taking cornering stiffness variations into account, we can represent the uncertain cornering stiffness as follows:

$$\begin{cases} k_f = k_{f,0} + \chi_f\tilde{k}_f \\ k_r = k_{r,0} + \chi_r\tilde{k}_r \end{cases} \tag{11}$$

where $k_{f,0}$ and $k_{r,0}$ are the nominal values of k_f and k_r, respectively. χ_f and χ_r are time-varying parameters, which satisfy $|\chi_{f/r}| \le 1$. Because that road conditions are usually uniform to the front and rear axles, we assume that $\chi_f = \chi_r$ to reduce the number of uncertainty parameters and computational burden. χ_f and χ_r are designed to illustrate tire nonlinear characteristics.

The state and control matrices in (7) can be modified based on (11)

$$\begin{cases} A(t) = A_0(t) + \Delta A(t) \\ B(t) = B_0(t) + \Delta B(t) \end{cases} \tag{12}$$

where $A_0(t)$ and $B_0(t)$ are the nominal values of matrices $A(t)$ and $B(t)$, respectively. $\Delta A(t)$ and $\Delta B(t)$ are the variation of matrices $A(t)$ and $B(t)$, respectively.

Many previous works proposed various steering controllers on the assumption of the vehicle constant speed. This article also takes into consideration of the time-varying parameter V_x. The polytopic uncertainty method is used to cover all the possible choices for V_x, and has been used in vehicle global chassis control [26], [27]. In general, we assume that vehicle longitudinal velocity V_x satisfy $v_{x,\min} \le V_x \le v_{x,\max}$. The longitudinal velocity varies in the range between $v_{x,\min}$ and $v_{x,\max}$. In this case, we define that

$$\begin{cases} v_{x,\max} = \overline{\xi}_1, v_{x,\min} = \overline{\xi}_2 \\ \frac{1}{v_{x,\min}} = \underline{\xi}_1, \frac{1}{v_{x,\max}} = \underline{\xi}_2. \end{cases} \tag{13}$$

We define that a polytopic uncertainty Ω could be described as the convex hull of a finite number of matrices $\upsilon_i$as

$$\begin{aligned} \Omega &= Co\{\upsilon_i, i = 1, 2, \ldots, l\} \\ &= \left\{ \sum_{i=1}^{l} a_i\upsilon_i : a_i \ge 0, \sum_{i=1}^{l} a_i = 1 \right\}. \end{aligned} \tag{14}$$

According to the polytopic uncertainty method, a polytope with $2^2 = 4$ vertices is utilized to cover all the possible choices for the uncertainty parameter pair $\{V_x\ 1/V_x\}$, and the vertices' coordination can be described as $\overline{\xi}_1, \overline{\xi}_2, \underline{\xi}_1, \underline{\xi}_2$. The time-varying parameters V_x and $1/V_x$ can be calculated by a summation of the vertices' coordinates as follows:

$$\begin{cases} V_x = \sum_{j=1}^{2} \overline{\varsigma}_j(t)\overline{\xi}_j \\ 1/V_x = \sum_{j=1}^{2} \underline{\varsigma}_j(t)\underline{\xi}_j \end{cases} \tag{15}$$

where $\widehat{\varsigma}_j$ and $\breve{\varsigma}_j$ denote the weighting factors of $\widehat{\xi}_j$ and $\breve{\xi}_j$, and they can be rewritten as

$$\begin{cases} \widehat{\varsigma}_1(t) = \frac{\widehat{\xi}_1 - V_x}{\widehat{\xi}_1 - \widehat{\xi}_2}, \widehat{\varsigma}_2(t) = \frac{V_x - \widehat{\xi}_2}{\widehat{\xi}_1 - \widehat{\xi}_2} \\ \breve{\varsigma}_1(t) = \frac{\breve{\xi}_1 - 1/V_x}{\breve{\xi}_1 - \breve{\xi}_2}, \breve{\varsigma}_2(t) = \frac{1/V_x - \breve{\xi}_2}{\breve{\xi}_1 - \breve{\xi}_2}. \end{cases} \tag{16}$$

Then, we define that

$$\varsigma_1 = \widehat{\varsigma}_1\breve{\varsigma}_1\ \varsigma_2 = \widehat{\varsigma}_1\breve{\varsigma}_2\ \varsigma_3 = \widehat{\varsigma}_2\breve{\varsigma}_1\ \varsigma_4 = \widehat{\varsigma}_2\breve{\varsigma}_2\,. \tag{17}$$

Based on the polytopic uncertainty method, we can rewrite the system plant, as shown in (8), in a polytopic form as

$$\begin{aligned} \dot{\mathbf{x}}(t) &= \sum_{j=1}^{4} \varsigma_j(t)[A_j\mathbf{x}(t) + Bu(t) + F_j w(t)] \\ &= \sum_{j=1}^{4} \varsigma_j(t)[(A_{0j} + \Delta A_j)\mathbf{x}(t) + (B_0 + \Delta B)u(t) + F_j w(t)] \end{aligned} \tag{18}$$

where the system, control, and interference matrices of each vertex $A_{0,j}$, F_j, and ΔA_j, and they can be calculated based on (15)–(17). Wherein $A_{0,j}$ denotes the system matrix with nominal cornering stiffness at each vertices.

Due to the definition, as shown in (17), we can obtain the following equation:

$$\sum_{j=1}^{4} \varsigma_j(t) = 1, \varsigma_j(t) \geq 0. \tag{19}$$

Moreover, based on the definition of ΔA_j and ΔB, they can be calculated as follows:

$$\begin{cases} \Delta A_j = \Gamma\Lambda\Theta_{1j} \\ \Delta B = \Gamma\Lambda\Theta_2 \end{cases} \tag{20}$$

where

$$\Gamma = \begin{bmatrix} 0\,0\,0\,1 \\ 0\,0\,1\,0 \end{bmatrix}^T, \Lambda = \begin{bmatrix} \lambda_f & 0 \\ 0 & \lambda_f \end{bmatrix}, \Theta_2 = \begin{bmatrix} \frac{\tilde{k}_f}{m} \\ \frac{\tilde{k}_f l_f}{I_z} \end{bmatrix},$$

$$\Theta_{1j} = \begin{bmatrix} 0\,0 & \frac{(\tilde{k}_f + \tilde{k}_r)\breve{\xi}_j}{m} & \frac{(\tilde{k}_f l_f - \tilde{k}_r l_r)\breve{\xi}_j}{m} \\ 0\,0 & \frac{(\tilde{k}_f l_f - \tilde{k}_r l_r)\breve{\xi}_j}{I_z} & \frac{(l_f^2\tilde{k}_f + l_r^2\tilde{k}_r)\breve{\xi}_j}{I_z} \end{bmatrix}. \tag{21}$$

The vehicle path tracking model can be rewritten in a discrete form by combining (18) and (20) as follows:

$$\begin{aligned} \mathbf{x}(k+1) &= \sum_{j=1}^{4} \varsigma_j(k)[\bar{A}_j\mathbf{x}(k) + \bar{B}u(k) + f(k)] \\ \bar{A}_j &= A_{0j} + \Gamma\Lambda\Theta_{1j}, \bar{B} = B_0 + \Delta B, f(k) = F_j w(k) \end{aligned} \tag{22}$$

where $f^T(k)f(k)$ satisfies that $f^T(k)f(k) < \beta_0^2 x^T(k)x(k)$, β_0 is a positive constant.

III. LMI-Based MPC Controller Design

A. Problem Formulations and Preliminaries

This article aims to design a robust LMI-based MPC, which is robust against tire cornering stiffness uncertainty and time-varying vehicle speed. The uncertain system plant we concerned is as shown in (22), and its states are measurable. The robust LMI-based MPC can be described in the following optimization problem, which minimizes the worst case infinite horizon quadratic objective function:

$$J_\infty(k) = \sum_{i=0}^{\infty} \left[\|x(k+i|\,k)\|_{W_x}^2 + \|u(k+i|\,k)\|_{W_u}^2 \right] \tag{23}$$

$$\min_{u(k+i|k),i\geq 0} \max_{[\bar{A}(k+i),\bar{B}(k+i)]\in\Omega, i\geq 0} J_\infty(k)$$

$$\text{s.t. } \|u(k+i\,|k)\| \leq u_{\max} \quad \forall i \geq 0, k \geq 0 \tag{24}$$

where $x(k+i|k)$ and $u(k+i|k)$ denote the state predicted based on the measurements and the control input at time $k+i$, computed at time k, respectively. Besides $x(k) = x(k|k)$ and $u(k) = u(k|k)$ denote the measured state and control input applied to the system plant at time k, respectively. W_x and W_u are weighting matrices of system states (the items of W_x corresponding to V_y and φ are zero) and control input, respectively, and they are symmetrical positive-definite and semidefinite matrices. The value of $u_{\max}$ is set based on vehicle steering system characteristics, and its value is considered in the algorithm design. The maximization in (24) is taken over the set Ω of uncertain systems.

B. Design of the LMI-Based MPC Controller

A state feedback control law is designed for the system plant in (22) as follows:

$$u(k+i\,|k) = Kx(k+i\,|k) \tag{25}$$

where K denotes the gain matrix, which ensures the asymptotic stability of the closed-loop system of the concerned system plant. The following discussion describes the derivation of the designed gain matrix.

According to the abovementioned optimization problem in (23) and (24), the designed state feedback law should satisfy the following conditions:

$$\begin{cases} J\infty(k) < \gamma \\ \|u(k+i\,|k)\| \leq u_{\max} \quad \forall i \geq 0, k \geq 0 \end{cases} \tag{26}$$

where γ is an upper bound on $J_\infty(k)$.

A Lyapunov–Krasovskii quadratic function at time k is defined as

$$V(x(k)) = x^T(k)P_0x(k) \tag{27}$$

where P_0 is a symmetrical positive-definite matrix.

Supposing the defined Lyapunov–Krasovskii quadratic function satisfies the following equation:

$$\begin{aligned} V(k+i+1\,|k) - V(k+i\,|k) &\leq -l(x,u,i) \\ \forall [A(k+i)B(k+i)] &\in \Omega \end{aligned} \tag{28}$$

where $l(x,u,j) = \|x(k+i|k)\|^2_{W_x} + \|u(k+i|k)\|^2_{W_u}$. Requiring $x(\infty|k) = 0$ such that $V(\infty|k) = 0$.

Summing (28) from $i = 0$ to $i = \infty$, we could obtain the following equation:

$$-V(x(k\,|k)) \le -J_\infty(x(k\,|k)). \tag{29}$$

Therefore, an upper bound on $J_\infty(k)$ can be obtained

$$\max_{[\bar{A}(k+i),\bar{B}(k+i)]\in\Omega, i\ge 0} J_\infty(k) \le V(x(k\,|k)). \tag{30}$$

Thus, the state feedback control law $u(k+i|k) = Kx(k+i|k)$ can satisfy the condition in (26) if the defined Lyapunov–Krasovskii quadratic function satisfies the condition in (28).

Lemma 1. Both $W_0(x)$ and $W_1(x)$ are quadratic functions of $x \in R^n$. $\forall x \in R^n - \{0\}$, $W_1(x) < 0$ always holds. If there exists $\rho > 0$ such that $W_0(x) - \rho W_1(x) < 0, x \ne 0$, $W_0(x) < 0$ holds.

Theorem 1. The state feedback control law, as shown in (25), and the state feedback gain $K = YQ^{-1}$ could satisfy the performance objective, as shown in inequality (28), if there exist scalar $\gamma(k) > 0$, $\rho > 0$, symmetrical positive-definite matrices Q and P_0, and a matrix Y of appropriate dimension, which satisfies the following LMI optimization problem:

$$\min_{\gamma(k),Y,\rho,Q,P_0} \operatorname{tr}(\operatorname{diag}\{P_0, I_n\}) \tag{31}$$

s.t.

$$\begin{pmatrix} \operatorname{diag}(\gamma(k),\gamma(k)) & \operatorname{diag}(x^T(k)P_0^T, f^T(k)I_n) \\ \operatorname{diag}(P_0x(k), f(k)I_n) & \operatorname{diag}(P_0, I_n) \end{pmatrix}_{10\times 10} \ge 0, \tag{32}$$

$$\begin{bmatrix} u^2_{\max} & Y \\ Y^T & Q \end{bmatrix} \ge 0 \tag{33}$$

$$\begin{pmatrix} N_{00} & 0 & (\bar{A}_jQ + \bar{B}_jY)^T \\ 0 & -\rho I_n & 0 \\ \bar{A}_jQ + \bar{B}_jY & 0 & -Q \end{pmatrix}_{21\times 21} < 0 \quad j = 1,2,3,4 \tag{34}$$

$$N_{00} = \begin{pmatrix} -Q & * & * & * \\ \beta_0 Q & -\frac{1}{\rho}I_n & * & * \\ W_x^{1/2}Q & 0 & -\gamma(k)I_n & * \\ W_u^{1/2}Y & 0 & 0 & -\gamma(k) \end{pmatrix}_{13\times 13} \tag{35}$$

with $*$ denotes the symmetric element of the matrix, and $\operatorname{tr}(\Phi)$ represents the trace of the matrix Φ. I_n is an n-dimensional unit matrix. $\operatorname{diag}(\iota_1, \iota_2, \ldots, \iota_n)$ denotes a diagonal matrix with the diagonal element ι_i.

Proof. The input constraint can be incorporated into our robust MPC algorithm as sufficient LMI constraints. Based on (26) and (25), we have

$$\max_{i\ge 0} \|u(\,k+i|\,k)\|^2 = \max_{i\ge 0} \left\|YQ^{-1}x(\,k+i|\,k)\right\|^2. \tag{36}$$

Based on the Schur complement lemma, the following LMI in Y and Q, as shown in (33), must hold so that the input constraint $\|u(k+i|k)\|^2 \le u^2_{\max}$ is satisfied [29].

$V(x(k))$ is an upper bound of $J_\infty(x(k))$, and it can be minimized through solving the following problem:

$$\min_{\gamma(k),Y,\rho,Q,P_0} \operatorname{tr}(\operatorname{diag}\{P_0, I_n\})$$

s.t.

$$w^T(k)Pw(k) \le \gamma(k) \tag{37}$$

where $w(k) = [\,x^T(k)\ f^T(k)\,]^T$, $P = \operatorname{diag}(P_0, I_n)$.

Based on the Schur complement lemma, the inequality $w^T(k)Pw(k) \le \gamma(k)$ can be rewritten as follows:

$$\begin{pmatrix} \gamma(k) & w^T(k) \\ w(k) & P^{-1} \end{pmatrix} \ge 0. \tag{38}$$

Multiplying the inequality (38) from the left-hand side by $\operatorname{diag}(I_n, P)$ and from the right-hand side by $\operatorname{diag}(I_n, P)$, we can obtain

$$\begin{pmatrix} \gamma(k) & w^T(k)P^T \\ Pw(k) & P \end{pmatrix} \ge 0. \tag{39}$$

Therefore, the inequality (32) holds.

Combining $u(k+i|k) = Kx(k+i|k), i \ge 0$ and the system plant in (22), the derivatives of the Lyapunov–Krasovskii quadratic function can be obtained

$$\begin{aligned} \Delta V(x(k)) &= V(x(k+1)) - V(x(k)) \\ &= w^T(k)(\Psi_1 + \Pi_1^T P \Pi_1)w(k) \end{aligned} \tag{40}$$

where the matrices Ψ_1, Π_1 are presented as follows:

$$\begin{cases} \Psi_1 = \operatorname{diag}\{-P_0\ \mathbf{0}\} \\ \Pi_1 = \operatorname{diag}\{A + BK\ I_n\}. \end{cases} \tag{41}$$

We define $W_0(x)$ such that

$$W_0(x) = \Delta V(x(k)) + l(x,u,i). \tag{42}$$

Based on (40), we can rewrite $W_0(x)$ as follows:

$$W_0(k) = w^T(k)(\Psi_2 + \Pi_1^T P \Pi_1)w(k) \tag{43}$$

where $\Psi_2 = \operatorname{diag}\{-P_0 + K^TW_uK + W_x\ \mathbf{0}\}$.

Based on the condition $f^T(k)f(k) < \beta_0^2 x^T(k)x(k)$, we can derive the following inequality:

$$W_1(k) = w^T(k)\Psi_3 w(k) < 0 \tag{44}$$

where $\Psi_3 = \operatorname{diag}\{-\beta_0^2 I_n\ I_n\}$.

Based on Lemma 1, $W_0(k) < 0$ if the following condition holds:

$$\begin{aligned} &W_0(k) - \lambda W_1(k) < 0 \\ &\Rightarrow w^T(k)(\Psi_2 + \Pi_1^T P \Pi_1)w(k) - \lambda w^T(k)\Psi_3 w(k) < 0. \end{aligned} \tag{45}$$

Cancelling the common factor $w^T(k)w(k)$ of the inequality (45), we can obtain

$$\Psi_2 + \Pi_1^T P \Pi_1 - \lambda \Psi_3 < 0 \tag{46}$$

where λ is a positive constant.

Define that $Q = \gamma(k)P_0^{-1}$. By the Schur complement, (46) is equivalent to the following inequality:

$$\begin{pmatrix} \Theta_{00} & 0 & (A+BK)^T \\ 0 & -\rho I_n & 0 \\ A+BK & 0 & -Q \end{pmatrix} < 0 \tag{47}$$

where $\Theta_{00} = -Q^{-1} + \gamma^{-1}(k)(W_x + K^T W_u K) + \rho\beta_0^2 I_n$, and $\rho = \gamma^{-1}(k)\lambda$.

Multiplying the inequality (47) from the left-hand side and right-hand side by $\mathrm{diag}\{\, Q \; I_n \; I_n \,\}$, and substituting $Y = KQ$ into it, we get

$$\begin{pmatrix} \tilde{\Theta}_{00} & 0 & (AQ+BY)^T \\ 0 & -\rho I_n & 0 \\ AQ+BY & 0 & -Q \end{pmatrix} < 0 \tag{48}$$

where $\tilde{\Theta}_{00} = -Q + \gamma^{-1}(k)QW_xQ + \gamma^{-1}(k)Y^TW_uY + \rho\beta_0^2 QQ$.

Then, applying the Schur complement lemma again to the inequality (48), we get

$$\begin{pmatrix} N_{00} & 0 & (AQ+BY)^T \\ 0 & -\rho I_n & 0 \\ AQ+BY & 0 & -Q \end{pmatrix} < 0 \tag{49}$$

where

$$N_{00} = \begin{pmatrix} -Q & * & * & * \\ \beta_0 Q & -\frac{1}{\rho} I_n & * & * \\ W_x^{1/2} Q & 0 & -\gamma(k) I_n & * \\ W_u^{1/2} Y & 0 & 0 & -\gamma(k) I_n \end{pmatrix}. \tag{50}$$

According to the polytopic uncertainty method, the inequality (50) holds if and only if it holds at each matrix υ_i of the convex hull, that is the inequality (50) holds if and only if the inequality (34) holds. Then, the gain matrix K_j of each matrix υ_i can be optimized based on the abovementioned Theorem 1. The resulting solution remains the same except that K_j replaces K, so the state feedback control law can be obtained as follows:

$$u(k) = \sum_{j=1}^{4} \varsigma_j(k) K_j x(k). \tag{51}$$

C. Robust Stability Offline LMI-Based MPC

The proposed Algorithm 1 costs much online computation when the system plant is a one high-order system or has parameters with fast changes. Therefore, in this section, an offline approach based on the concept of the asymptotically stable invariant ellipsoid is presented [30]. The subsequent offline formulation of the system, as shown in (22), is illustrated.

Algorithm 1: The Main Steps of Our Proposed LMI-Based MPC Path-Tracking Controller Are Shown as Follows.

LMI-based MPC path-tracking controller

1. Get the measured state $x(k)$
2. Select the appropriate matrices W_x and W_u
3. Initialize all the variables used in (31)–(34), including $\gamma(k)$, ρ, Q, P_0, and Y
4. Obtain all the defined variables in step three by solving the optimization problem, as shown (31)–(34)
5. Calculate the state feedback gain matrix $K = YQ^{-1}$
6. Apply $u(k) = \sum_{j=1}^{4} \varsigma_j(k) K_j x(k)$ to the process
7. Set $k := k+1$ and go to step 1

First, the asymptotically stable invariant ellipsoid is defined as follows. There exist a discrete dynamical system $x_a(k+1) = f(x_a(k))$, and an asymptotically stable invariant ellipsoid, which is a subset $\vartheta = \{x_a \in \Re^{n_x} | x_a^T Q_{x_a}^{-1} x_a \le 1\}$ of the state-space $\Re^{n_x}$. Whenever $x_a(k_1) \in \vartheta$, then $x_a(k) \in \vartheta$ for all times $k \ge k_1$ and $x_a(k) \to 0$ as $k \to \infty$.

Then, based on (26) and (30) in Theorem 1, i.e., $V(x(k|k)) \le \gamma$, the following equation holds, which is automatically satisfied for all states within the ellipsoid ϑ:

$$\begin{bmatrix} 1 & * \\ x(k\,|k) & Q \end{bmatrix} \ge 0, Q > 0. \tag{52}$$

Thus, the minimizer of Theorem 1 at a given state x_0 of the system plant in (22) is feasible but not necessarily optimal for any other state in ϑ. We can apply the state feedback law $u = YQ^{-1}x$ to any nonzero $\tilde{x}(k) \in \vartheta$, where $\tilde{x}(k) \ne x_0$ and still satisfy the inequation in Theorem 1, thereby ensuring that in real time the following inequation satisfies:

$$\begin{aligned} &\tilde{x}(k+i+1)^T Q^{-1} \tilde{x}(k+i+1) \\ &\quad < \tilde{x}(k+i)^T Q^{-1} \tilde{x}(k+i) \le 1, i \ge 0. \end{aligned} \tag{53}$$

Thus, $\tilde{x}(k+i) \in \vartheta, i \ge 0$ and $\tilde{x}(k+i) \to 0$ as $i \to \infty$, establishing that ϑ is an asymptotically stable invariant ellipsoid.

Therefore, we can adopt varying feedback matrices based on the asymptotically stable invariant ellipsoids one inside another to reduce the online computational burden. First, we set a series of state points $x_i, i = 1, 2, \ldots, N$. A sequence of minimizers $\gamma_i, \rho_i, Q_i, P_{0,i}, Y_i$, solutions of the LMI optimization problem in Theorem 1 can be obtained through the following steps.

Thus, the proposed LMI-based MPC path-tracking controller can work based on a set of states instead of a single state, so it is available offline due to the prereserved lookup table. Therefore, the computational burden of our proposed controller is very small and it can be applied practically to vehicle hardware.

Algorithm 2: Consider the Problem in Theorem 1, The Main Steps of the Offline Algorithm Are as Follows. Let $i := 1$.

Offline algorithm of path-tracking control

1. Compute the minimizer $\gamma_i, \rho_i, Q_i, P_{0,i}, Y_i$ at x_i by solving the LMI problem in Theorem 1 with an additional constraint $Q_{i-1} > Q_i$ (ignored at $i = 1$), store the obtained minimizer $\gamma_i, \rho_i, Q_i, P_{0,i}, Y_i$ in a lookup table.
2. If $i < N$, choose a state x_{i+1} which satisfies $\|x_{i+1}\|_{Q_i^{-1}} < 1$. Let $i := i + 1$, go to step 1.
3. When the system is controlled online, based on the state $x(k)$ at time k, we perform a bisection search over Q_i^{-1} in the lookup table to find the largest index i, i.e., the smallest ellipsoid ϑ_i. Then, apply the control law $u(k) = K_i x(k), K_i = Y_i Q_i^{-1}$

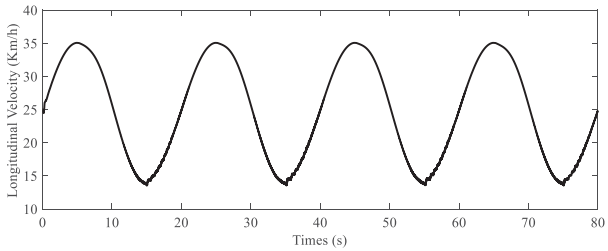

Fig. 2. Vehicle longitudinal velocity in the simulation test.

IV. Simulation and Experiment Results

The path tracking problem is formulated and solved through the LMI-based MPC controller in the aforementioned two sections. To validate the proposed path-tracking controller, MATLAB /Simulink cosimulation and real-bus experiment are performed, and results are analyzed. The main difference between a sedan car and a bus is the larger steering ratio of the bus steering system for path tracking problems. Based on the mechanical structure of the experimental bus's steering system, the range of steering wheel angle is set to –900°–900°.

A. Simulation Results

CarSim is a fidelity vehicle simulator, and is widely used in the automotive industry for vehicle handling stability and ride tests. In the simulation, the vehicle dynamics is totally provided by CarSim, and a D-class Sedan full-vehicle model is selected as the autonomous car to be controlled. An LPV-based MPC controller is used to be compared with the proposed path-tracking controller [36].

In simulation test scenarios, vehicle longitudinal velocity is time-varying, as shown in Fig. 2, and it fluctuates over time similar to a sine curve. The maximum and minimum speed is about 35 and 14 km/h, respectively. The desired path profile in the lane change maneuver is a simulated urban curved highway, as shown in Fig. 3, and it captures a variety of driving scenarios representative of real-world driving. Simulation results of the propose LMI-based MPC controller and the LPV-based MPC

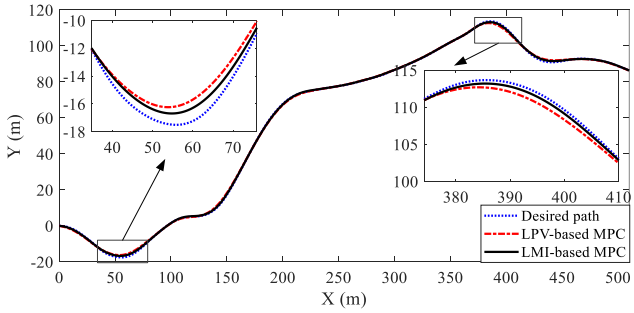

Fig. 3. Tracking performance comparison of the simulation test.

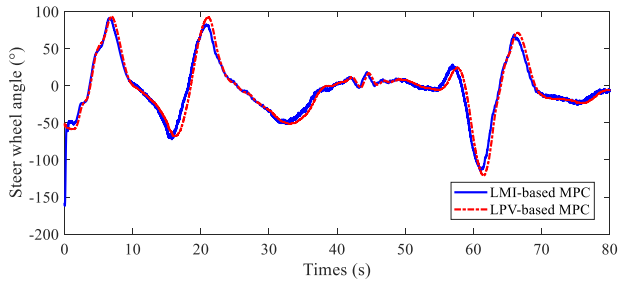

Fig. 4. Steer wheel angle comparison in the simulation.

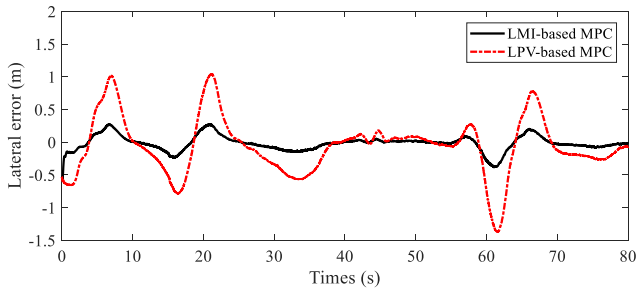

Fig. 5. Lateral error comparison in the simulation.

for the desired and actual road curvature, vehicle steering wheel angle, and lateral error are presented in Figs. 3–5.

As shown in Fig. 3, the actual trajectory controlled by LMI-based MPC tracks the desired trajectory exactly even through the vehicle speed varies from 14 to 35 km/h. While the actual trajectory controlled by the LPV-based MPC can track the desired trajectory, but the tracking error is a bit larger. The maximum lateral error controlled by the proposed LMI-based MPC is about 0.25 m at 61.2 s, when the vehicle steers sharply on the large bend road, but the maximum lateral error controlled by the LPV-based MPC is about 1.4 m, which is shown in Fig. 5. It can be found that the proposed controller has a strong robustness against the vehicle time-varying speed. The proposed path tracking controller can limit the tracking lateral error into an accepted magnitude, which demonstrates that the trajectory tracking performance can be guaranteed effectively. Comparison of the steer wheel angle controlled by the two algorithms is presented in Fig. 4, and the values controlled by the LMI-based MPC are maintained in normal regions. The maximum value of

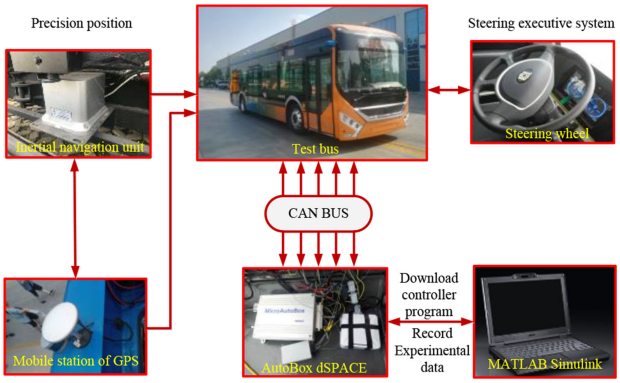

Fig. 6. Experiment bus with various sensors and equipment.

Fig. 7. Path tracking scenario in the experimental test.

the steer wheel angle is about –113.5 ° at 61 s, when the vehicle is turning on large bend road. At the same time.

We can find that the path tracking maneuver on the simulated urban curved highway is finished satisfactorily, with a smaller tracking error. Considering the path tracking simulation is carried out with time-varying longitudinal velocity, the proposed path tracking controller's effectiveness and robustness is validated.

B. Experiment Results

In order to further visualize the effectiveness of the proposed path tracking controller, real bus experimental test with time-varying vehicle velocity is performed by the LCK6105GZ bus of Zhongtong Bus Holding Co., Ltd. Its total vehicle mass is 12 000 kg, and the values of its length, width, and height are 10.5, 2.55, and 2.98 m, respectively.

As shown in Fig. 6, the real-bus test is conducted on our experiment platform to verify the proposed system's performance, and it is equipped with the visual camera, high-precision differential GPS, inertial navigation unit, and MicroAutoBox dSPACE, etc. According to the upper controller's command, the drive and brake systems are controlled by the vehicle unit (VCU), and the steering system implements corresponding steering angles. The control algorithm built in MATLAB/Simulink runs in the MicroAutoBox dSPACE with the 0.01 s sample time.

Fig. 7. presents the experimental scenario. The test scenario is conducted in Zhongtong Bus Holding Co., Ltd, Shandong, China, whose satellite map is shown in Fig. 7. The total mileage

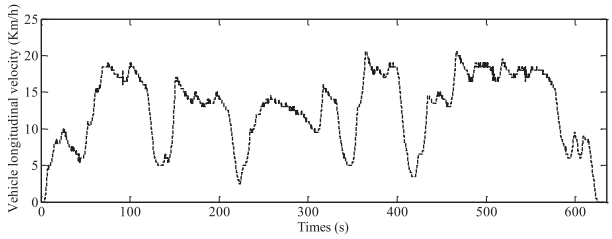

Fig. 8. Test bus longitudinal velocity in the experimental test.

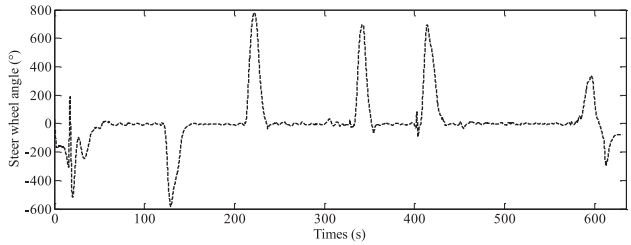

Fig. 9. Steer wheel angle in the experimental test.

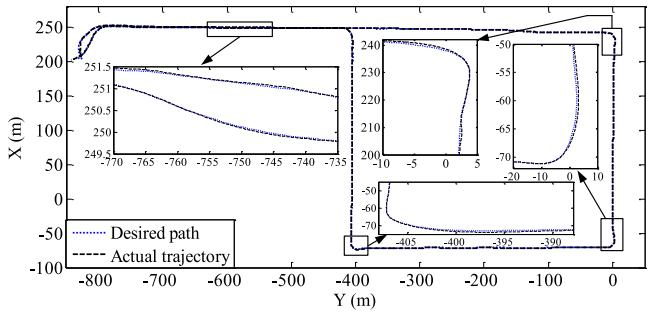

Fig. 10. Tracking performance of the experimental test.

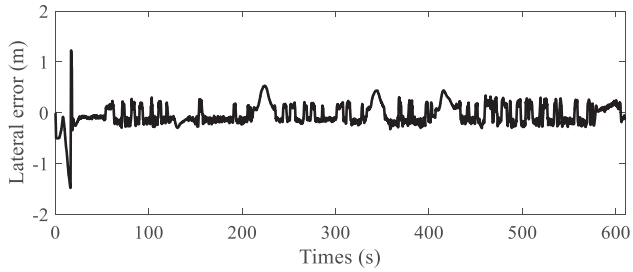

Fig. 11. Lateral error in the experimental test.

of the experiment is about 2.2 km, and the desired trajectory is a road course around Zhongtong Bus production and assembly workshop. Vehicle longitudinal velocity fluctuates from 0 to about 21 km/h, as shown in Fig. 8.

The experimental results are presented in Figs. 9–11. It can be found that the values of the steer wheel angle are maintained in normal regions. As shown in Fig. 9, the whole road course has four big corners, and the value of vehicle steer wheel angle suddenly becomes pretty large at the big corners. The maximum value of the vehicle steer wheel angle is about 781.2 ° at 222 s.

The vehicle steer wheel angle in the experimental test is pretty large due to large steering ratio of the bus steering system. Fig. 10 illustrates the actual and desired trajectories, and it shows that the proposed path tracking controller can accurately track the desired road course. As shown in Fig. 11, the maximum value of the lateral error is about 1.5 m at the beginning of the experiment due to the large initial location error and complex desired trajectory, and then the maximum of the lateral error is about 0.52 m at the time when the experiment bus runs at one angle turn. The lateral error is larger than that of the simulation result due to four angle turns of the experimental course. Moreover, the vehicle wheelbase and width of the experimental bus is larger than those of a common sedan car, so that the lateral error is larger in the experimental test.

V. Conclusion

This article developed an autonomous vehicle path tracking controller by the LMI-based MPC approach. Then, an experimental real bus platform was established to test the proposed controller's performance. Polytopic uncertainty method was used to cover all the possible choices for the time-varying vehicle speed, and the coefficient stiffness was modified. Thus, a LPV lateral model considering tire nonlinear characteristics and time-varying parameter was built. Based on Lyapunov asymptotic stability and the minimization of the worst case infinite horizon quadratic objective function, the MPC-based path-tracking controller can be designed through a set of LMI.

To validate the proposed controller, MATLAB /Simulink cosimulation and real-bus experiment were carried out. Results showed the effectiveness of the proposed controller, and it ensured control accuracy and strong robustness. Especially, it performed well in autonomous driving tests of the LCK6105GZ bus. However, some innovative algorithms for path tracking control may be studied to obtain better control result in future works. Some issues such as path-tracking in bad road conditions including rough or slippery roads, vehicle lateral and longitudinal integrated control still need to be researched in the future.

References

[1] E. Lagarde, "Road traffic injuries," in *Encyclopedia of Environmental Health*, J. O. Nriagu, Ed. Burlington, MA, USA: Elsevier, 2011, pp. 892–900.

[2] L. Li, G. Jia, J. Song, and X. Ran, "Research progress on vehicle dynamics stability control," *Chin. J. Mech. Eng.*, vol. 49, no. 24, pp. 95–107, 2013.

[3] X. Li, Z. Sun, D. Cao, D. Liu, and H. He, "Development of a new integrated local trajectory planning and tracking control framework for autonomous ground vehicles," *Mech. Syst. Signal Process.*, vol. 87, pp. 118–137, 2017.

[4] L. Li, G. Jia, J. Chen, H. Zhu, D. Cao, and J. Song, "A novel vehicle dynamics stability control algorithm based on the hierarchical strategy with constrain of nonlinear tyre forces," *Veh. Syst. Dyn.*, vol. 53, no. 8, pp. 1093–1116, 2015.

[5] L. Li, Y. Lu, R. Wang, and J. Chen, "A three-dimensional dynamics control framework of vehicle lateral stability and rollover prevention via active braking with MPC," *IEEE Trans. Ind. Electron.*, vol. 64, no. 4, pp. 3389–3401, Apr. 2017.

[6] Y. Lian, Y. Zhao, L. Hu, and Y. Tian, "Longitudinal collision avoidance control of electric vehicles based on a new safety distance model and constrained-regenerative-braking-strength-continuity braking force distribution strategy," *IEEE Trans. Veh. Technol.*, vol. 65, no. 6, pp. 4079–4094, Jun. 2016.

[7] S. E. Li, Q. Guo, L. Xin, B. Cheng, and K. Li, "Fuel-saving servo-loop control for an adaptive cruise control system of road vehicles with step-gear transmission," *IEEE Trans. Veh. Technol.*, vol. 66, no. 3, pp. 2033–2043, Mar. 2017.

[8] W. Wang and D. Zhao, "Evaluation of lane departure correction systems using a regenerative stochastic driver model," *IEEE Trans. Intell. Veh.*, vol. 2, no. 3, pp. 221–232, Sep. 2017.

[9] Y. Xia, F. Pu, S. Li, and Y. Gao, "Lateral path tracking control of autonomous land vehicle based on ADRC and differential flatness," *IEEE Trans. Ind. Electron.*, vol. 63, no. 5, pp. 3091–3099, May 2016.

[10] J. Ackermann, D. Odenthal, and T. Bünte, "Advantages of active steering for vehicle dynamics control," in *Proc. 32nd ISATA Automot. Mechatron. Des. Eng.*, pp. 263–270. [Online]. Available: http://citeseerx.ist.psu.edu/viewdoc/download?doi=10.1.1.31.1688&rep=rep1&type=pdf

[11] J. Wu, S. Cheng, B. Liu, and C. Liu, "A human-machine-cooperative-driving controller based on AFS and DYC for vehicle dynamic stability," *Energies*, vol. 10, no. 11, 2017, Art. no. 1737.

[12] H. Zhang and J. Wang, "Active steering actuator fault detection for an automatically-steered electric ground vehicle," *IEEE Trans. Veh. Technol.*, vol. 66, no. 5, pp. 3685–3702, May 2017.

[13] X. Wu, B. Zhou, G. Wen, L. Long, and Q. Cui, "Intervention criterion and control research for active front steering with consideration of road adhesion," *Veh. Syst. Dyn.*, vol. 56, no. 4, pp. 553–578, 2018.

[14] H. Zhang, X. Zhang, and J. Wang, "Robust gain-scheduling energy-to-peak control of vehicle lateral dynamics stabilisation," *Veh. Syst. Dyn.*, vol. 52, no. 3, pp. 309–340, 2014.

[15] X. J. Jin, G. Yin, and N. Chen, "Gain-scheduled robust control for lateral stability of four-wheel-independent-drive electric vehicles via linear parameter-varying technique," *Mechatronics*, vol. 30, pp. 286–296, 2015.

[16] J. Zhao, P. K. Wong, X. Ma, and Z. Xie, "Chassis integrated control for active suspension, active front steering and direct yaw moment systems using hierarchical strategy," *Veh. Syst. Dyn.*, vol. 55, no. 1, pp. 72–103, 2016.

[17] H. Guo, F. Liu, F. Xu, H. Chen, D. Cao, and Y. Ji, "Nonlinear model predictive lateral stability control of active chassis for intelligent vehicles and its FPGA implementation," *IEEE Trans. Syst., Man, Cybern., Syst.*, vol. 49, no. 1, pp. 2–13, Jan. 2019.

[18] W. Zhao, X. Qin, and C. Wang, "Yaw and lateral stability control of Automotive four-wheel steer-by-wire system," *IEEE/ASME Trans. Mechatron.*, vol. 23, no. 6, pp. 2628–2637, Dec. 2018.

[19] P. Setlur, J. R. Wagner, D. M. Dawson, and D. Braganza, "A trajectory tracking steer-by-wire control system for ground vehicles," *IEEE Trans. Veh. Technol.*, vol. 55, no. 1, pp. 76–85, Jan. 2006.

[20] Z. Sun, J. Zheng, Z. Man, H. Wang, and R. Lu, "Sliding mode-based active disturbance rejection control for vehicle steer-by-wire systems," *IET Cyber-Phys. Syst., Theory Appl.*, vol. 3, no. 1, pp. 1–10, 2018.

[21] T. Ming, W. Deng, S. Zhang, and B. Zhu, "MPC-based trajectory tracking control for intelligent vehicles," 2016. [Online]. Available: http://dx.doi.org/10.4271/2016-01-0452

[22] G. V. Raffo, G. K. Gomes, J. E. Normey-Rico, C. R. Kelber, and L. B. Becker, "A predictive controller for autonomous vehicle path tracking," *IEEE Trans. Intell. Transp. Syst.*, vol. 10, no. 1, pp. 92–102, Mar. 2009.

[23] A. El Hajjaji and S. Bentalba, "Fuzzy path tracking control for automatic steering of vehicles," *Robot. Auton. Syst.*, vol. 43, no. 4, pp. 203–213, 2003.

[24] C.-L. Hwang, C.-C. Yang, and J. Y. Hung, "Path tracking of an autonomous ground vehicle with different payloads by hierarchical improved fuzzy dynamic sliding-mode control," *IEEE Trans. Fuzzy Syst.*, vol. 26, no. 2, pp. 899–914, Apr. 2018.

[25] Z. Fan and H. Chen, "Study on path following control method for automatic parking system based on LQR," *SAE Int. J. Passenger Cars—Electron. Electr. Syst.*, vol. 10, no. 1, pp. 41–49, 2016.

[26] C. Poussot-Vassal, *Robust LPV Multivariable Automotive Global Chassis Control*. Grenoble, France: Institut National Polytechnique de Grenoble - INPG, 2008.

[27] A. Zin, O. Sename, P. Gaspar, L. Dugard, and J. Bokor, "Robust LPV—∞ control for active suspensions with performance adaptation in view of global chassis control," *Veh. Syst. Dyn.*, vol. 46, no. 10, pp. 889–912, 2008.

[28] C. Poussot-Vassal, O. Sename, S. Fergani, M. Doumiati, and L. Dugard, "Global chassis control using coordinated control of braking/steering actuators," in *Robust Control and Linear Parameter Varying Approaches: Application to Vehicle Dynamics*, O. Sename, P. Gaspar, and J. Bokor, Eds. Berlin, Germany: Springer, 2013, pp. 237–265.

[29] M. V. Kothare, V. Balakrishnan, and M. Morari, "Robust constrained model predictive control using linear matrix inequalities," *Automatica*, vol. 32, no. 10, pp. 1361–1379, 1996.

[30] Z. Wan and M. V. Kothare, "An efficient off-line formulation of robust model predictive control using linear matrix inequalities," *Automatica*, vol. 39, no. 5, pp. 837–846, 2003/05/01/ 2003.
[31] M. H. Khooban, N. Vafamand, T. Niknam, T. Dragicevic, and F. Blaabjerg, "Model-predictive control based on Takagi-Sugeno fuzzy model for electrical vehicles delayed model," *IET Elect. Power Appl.*, vol. 11, no. 5, pp. 918–934, [Online]. Available: https://digital-library.theiet.org/content/journals/10.1049/iet-epa.2016.0508
[32] C. Chen, Y. Jia, M. Shu, and Y. Wang, "Hierarchical adaptive path-tracking control for autonomous vehicles," *IEEE Trans. Intell. Transp. Syst.*, vol. 16, no. 5, pp. 2900–2912, Oct. 2015.
[33] C. Zhang, J. Hu, J. Qiu, W. Yang, H. Sun, and Q. Chen, "A novel fuzzy observer-based steering control approach for path tracking in autonomous vehicles," *IEEE Trans. Fuzzy Syst.*, vol. 27, no. 2, pp. 278–290, Feb. 2018.
[34] S. Cheng, L. Li, and J. Chen, "Fusion algorithm design based on adaptive SCKF and integral correction for side-slip angle observation," *IEEE Trans. Ind. Electron.*, vol. 65, no. 7, pp. 5754–5763, Jul. 2018.
[35] J. Guo, Y. Luo, and K. Li, "Robust gain-scheduling automatic steering control of unmanned ground vehicles under velocity-varying motion," *Veh. Syst. Dyn.*, vol. 57, no. 4, pp. 595–616, 2019.
[36] J. W. Gong, Y. Jiang, and W. Xu, *Model Predictive Control for Self-Driving Vehicles*. Beijing, China: Beijing Institute of Technology Press, 2014.

Shuo Cheng received the B.S. degree in mechanical engineering from the Harbin Institute of Technology, Harbin, China, in 2016. He is currently working toward the Ph.D. degree in mechanical engineering with the Department of Automotive Engineering, Tsinghua University, Beijing, China.

His current research interests include intelligent vehicle chassis electronic control, vehicle dynamics domain control, and intelligent vehicle systems.

Liang Li (Senior Member, IEEE) received the Ph.D. degree in mechanical engineering from the Department of Automotive Engineering, Tsinghua University, Beijing, China, in 2008.

Since 2017, he has been a Tenured Professor with Tsinghua University. From November 2011 to December 2012, he was a Researcher with the Institute for Automotive Engineering, RWTH Aachen University, Aachen, Germany. His current research interests mainly include vehicle dynamics and control, adaptive and nonlinear system control, and hybrid vehicle develop and control.

Prof. Li is currently an Associate Editor for *IET Intelligent Transport System*, *PLOS ONE*, etc. He received the China Automotive Industry Science and Technology Progress Award for his achievements in the hybrid electrical bus in 2012, and the National Science Fund for Excellent Young Scholars of the People's Republic of China in 2014.

Xiang Chen received the B.S. degree in mechanical engineering from Hunan University, Changsha, China, in 2010, and the Ph.D. degree in vehicle engineering from the College of Automotive Engineering, Jilin University, Changchun, China, in 2018.

He is currently a Postdoctor with the Department of Automotive Engineering, Tsinghua University, Beijing, China. His current research interests mainly include vehicle dynamics and control, and hybrid electric vehicle develop and control.

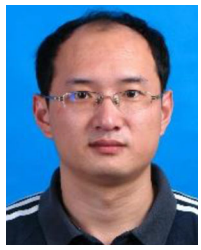

Jian Wu received the Ph.D. degree in vehicle engineering from the Nanjing University of Aeronautics and Astronautics, Nanjing, China, in 2015.

He was a Postdoctoral Researcher with the State Key Laboratory of Automotive Safety and Energy, Tsinghua University, Beijing, China, between 2016 and 2018. He is now an Associate Professor with the School of Mechanical and Automotive Engineering, Liaocheng University, Liaocheng, China.

He presided over a foundation for postdoctoral research in China, a natural science foundation for youth in Shandong province, and participated in the 863 program of national key natural science foundation. His current research interests include Key technologies of intelligent driving, steering system based on PMSM motor, and intelligent driving assistance system hardware in the loop technology.

Dr. Wu is the Reviewer of journals such as the *Journal of Automobile Engineering*, *International Journal of Vehicle design*, IEEE TRANSACTIONS ON INDUSTRY ELECTRONICS, and IEEE TRANSACTIONS ON HUMAN MACHINE SYSTEM.

Hong-da Wang received the B.S. degree in mechanical and electronic engineering from the Qinghai university, Qinghai, China, in 2015.

He is currently with the Zhongtong Bus Co., Ltd, Liaocheng, China. His current research interests include vehicle intelligent network connection and vehicle electrical design.